

Are some nanotwinned fcc metals optimal for strength, ductility and grain stability?

Yashashree Kulkarni^{a,*}, Robert J. Asaro^b

^a Department of Mechanical Engineering, University of Houston, Houston, TX 77204, USA

^b Department of Structural Engineering, University of California, San Diego La Jolla, CA 92093, USA

Received 26 February 2009; received in revised form 6 May 2009; accepted 28 June 2009

Available online 28 July 2009

Abstract

Here we investigate whether certain face-centered cubic metals display a superior behavior of nanotwinned structures compared to others. We also address the question of an optimal lamella thickness that yields maximum strength and stability. Our analysis of the intrinsic stacking fault energies, γ_{sf} , and the unstable stacking fault energies, γ_{us} , of Al, Pd, Cu and Ag, as well as our atomistic simulations of dislocation–twin boundary interactions in these metals, suggests an optimal behavior of nanotwinned Pd and Ag as competitive to Cu, and hence a special utility in their synthesis and further exploration. Our results also indicate that the influence of twin–twin interactions may lead to a loss of strength below a critical value of twin lamella thickness.

© 2009 Acta Materialia Inc. Published by Elsevier Ltd. All rights reserved.

Keywords: Nanotwins; Grain stability; Nanocrystalline metals

1. Introduction

It has long been established that twin boundaries are strong barriers to dislocation motion and thus constitute an effective structural strengthening motif [1]. The shear strength of coherent twin boundaries is also known to be relatively high as compared to, for example, other symmetric boundaries such as symmetric tilt boundaries [2]. Moreover, twin boundaries are of very low energy [1] – and most specifically, in the present context, of low energy as compared to tilt boundaries or boundaries of random orientation – and thus are stable since energetic driving forces promoting their removal are minimal. Thus it is unsurprising that recent efforts aimed at the synthesis of nanotwinned face-centered cubic (fcc) metals have demonstrated that

nanotwinned Cu displays an excellent array of mechanical properties [3,4]. Against the backdrop of the fact that nanocrystalline metals are known to be mechanically unstable – i.e. when subjected to very high stresses and deformation they undergo grain coarsening [5,6] and thereby lose their high strength – attention has focused on a fundamental understanding of the mechanisms mediating the behavior of nanotwinned metals. Indeed preliminary inquiries into nanotwin structural stability have been reported by Shute et al. [7] in Cu subject to cyclic deformation and indicate the greater stability of the nanotwinned structure as compared to a nanocrystalline counterpart. In fact, Kulkarni et al. [8] posed the question of whether or not nanotwinned structures in fcc metals were optimal regarding stability and strength via atomistic simulations. They concluded that when compared to strengthening by other types of boundaries, nanotwinned structures were indeed optimal. By nanotwinned metals we refer herein to fcc metals containing twins with lamella spacings below 100 nm. Nanotwinned fcc metals possess high strength and high sensitivity to strain rate, competitive with the strength of their nanocrystalline counterparts [9,10].

* Corresponding author. Address: University of Houston, Department of Mechanical Engineering, Engineering Building 1, 4800 Calhoun Rd, Houston, TX 77204 4006, United States. Tel.: +1 713 743 3657; fax: +1 713 743 4503.

E-mail address: ykulkarni@uh.edu (Y. Kulkarni).

Complete documentation of the stability of nanotwinned structures remains an open issue. Yet another question is whether certain fcc metals display superior behavior when compared to others and are thus optimal. Further, is there an optimal structure in a given fcc metal in terms of lamella thickness that gives optimal strength and stability? It is these latter questions we address herein as a prelude for developing processing routes for synthesizing truly bulk forms of nanotwinned metals. Accordingly, we study the interaction of dislocations, generated by molecular dynamics simulations of nanoindentation, in four fcc metals, Al, Cu, Pd and Ag, that vary both in elastic moduli and fault energies. Fault energies considered important to the dislocation–twin interaction processes are the intrinsic stacking fault energy, γ_{sf} , and the unstable fault energy, γ_{us} , the energy barrier associated with the formation of a Schockley partial dislocation. We also explore the influence of twin–twin interactions that may lead to significant loss of strength when the twin lamella thickness falls below a critical value. This has the effect of setting a maximum strength for nanotwinned fcc metals.

2. Background and perspectives

Following the experimental studies of Lu and co-workers [3,9], Asaro and Kulkarni [11] posed several specific questions regarding the properties listed above. They established a mechanistic basis for the high sensitivity to strain rate based on models describing dislocation absorption and/or transmission into, or across, twin boundaries. They showed that the processes involved in dislocation–twin boundary interaction indeed lead to rather low activation volumes, and thereby to high rate sensitivity and high resistance, and thus high strength. Their models also contain a natural description of the effect of twin lamellae thickness on both rate sensitivity and strength. Similar conclusions, at least regarding rate sensitivity, were reached by Zhu et al. [12] who used molecular dynamics to study the interaction of pure idealized infinitely straight screw dislocations with a twin boundary. The past several years have seen a number of studies exploring the interaction of dislocations with twin boundaries, essentially all focused on

simulating idealized, isolated, infinitely straight segments of dislocations driven to impinge on a twin interface [13–16]. Such simulations do not address questions of nucleation events per se, but instead focus on trying to understand the interplay between processes of dislocation absorption and/or transmission through the twin interface. Attempts had been made in some of these studies to correlate the nature of interaction, i.e. transmission vs. absorption, with parameters based on the relative values of lattice fault energies as used by Rice [17] in an analysis of dislocation emission from a crack tip – this will be addressed below in connection with Fig. 1, since however useful this may be, the original analysis was never meant to apply to the process of dislocation twin boundary interaction under consideration here. Before doing this, however, we add an additional note of perspective.

Lu et al. [4] have reported that when nanotwinned Cu is synthesized by pulsed electrodeposition, the strength increases with decreasing lamella thickness, λ , down to $\lambda \sim 15$ nm. When the lamella thickness falls below 15 nm, the strength significantly decreases. The high-resolution transmission electron microscopy (HRTEM) performed by Lu et al. [4] indicated that twin boundaries contained a density of Shockley partial dislocations nearly independent from the twin density, i.e. the twin lamellar thickness, and that the Burgers vector of these partial dislocations lay in the twin plane. The partial dislocations were thereby mobile and could render the twin plane a sort of slip system in itself. Thus as the lamella thickness decreases, and the density of potentially active twin planes increases, their contribution to yielding and deformation increases. The manifestation of this is a decreasing yield stress. Interestingly, Asaro and Kulkarni's [11] study of dislocation–twin boundary interactions indicated that the strengthening effect of nanotwin lamella would saturate at a twin lamella thickness of about 20 nm or just below. In fact, their model analysis showed that the strengthening effect of decreasing lamella thickness would scale as $\lambda^{-1/2}$ but at such small lamella thickness the effect would saturate for the simple reason that at $\lambda \sim 15$ –20 nm there can be no further reduction in the number of dislocations (or partial dislocations) piled up within a given twin lamella (see Fig. 1c). Thus

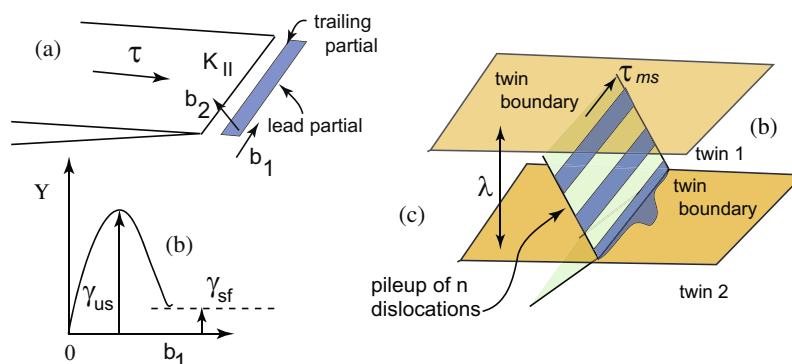


Fig. 1. Schematic for (a) the emission of a dislocation from a crack tip, (b) the generalized stacking fault energy curve, and (c) the process of cross-slip of a dislocation onto a twin plane due to a pile up of dislocations in the bulk crystal.

below $\lambda \sim 15$ nm or so, the yield strength would appear to decrease with further twin lamella thickness at a given strain rate as the density of twin boundaries increases. Kulkarni et al. [8] indeed found in their simulations that partial dislocations are mobile within twin boundaries as Lu et al. [4] suggest in their argument. This effect is explored in more detail below.

Rice [17] analyzed the process of the emission of perfect and partial dislocations from a crack tip, and this analysis served as a basis for considering the ductile to brittle transition in crystalline materials. A simple case is depicted in Fig. 1a, which shows an extended dislocation emitted on the crack plane. The process first involves the emission of the lead partial considered in this example to have a Burgers vector co-linear with the crack front. There is a critical condition defined by a critically large value of the crack stress intensity factor indicated for a Mode II scenario as K_{II} . Following this critical event, there is the second step of emitting the trailing partial which has a second critical condition associated with it. The emission of the lead partial is associated with the energy landscape sketched in Fig. 1b wherein during slip process b_1 the energy rises from 0 to a peak at γ_{us} and then falls to γ_{sf} , where γ_{us} and γ_{sf} are the so-called unstable stacking energy and the intrinsic stacking fault energy, respectively. Rice's analysis, applied to this particular scenario, gives the critical condition as:

$$K_{II}^{\text{crit}} = \sqrt{\frac{2\mu\gamma_{us}}{1-\nu}}, \quad (1)$$

where μ and ν are the shear modulus and the Poisson ratio, respectively. To emit the trailing partial, b_2 , Rice notes that the existence of the lead partial, b_1 , has set the energy level to γ_{sf} and thus the energy barrier to be surmounted is now $\gamma_{us} - \gamma_{sf}$. When the crack loading is pure Mode II, as we are considering here, the new criterion is:

$$K_{II}^{\text{crit}} = \sqrt{2\mu[(4-3\nu)\gamma_{us} - 3(1-\nu)\gamma_{sf}]/(1-\nu)}. \quad (2)$$

There are no values of ν for which the coefficient of γ_{us} within the radical is equal to that of γ_{sf} , but for $\nu = 1/3$, for instance:

$$K_{II}^{\text{crit}} = \sqrt{3\mu[3\gamma_{us} - 2\gamma_{sf}]}. \quad (3)$$

When the crack is loaded in a mixed mode involving Mode III as well, Rice notes that the required increase in K_{II} vanishes if:

$$K_{III}^{\text{crit}} = \sqrt{2\mu(\gamma_{us} - \gamma_{sf})/(1-\nu)}(\sqrt{4-3\nu}-1)/\sqrt{3}, \quad (4)$$

where this is obtained by setting K_{II} equal to its critical value for emission of the lead partial dislocation. Thus we arrive at the point of saying that for the emission of a complete dislocation we have in general a criterion that quite approximately says that:

$$K^{\text{crit}} \propto \sqrt{\mu\gamma_{us}}\sqrt{1-\gamma_{sf}/\gamma_{us}} = \beta^{1/2}\sqrt{\mu\gamma_{us}}. \quad (5)$$

The criterion contains two rather different contributions, namely a scale factor involving the product of shear modulus and unstable stacking energy, $\mu\gamma_{us}$, and the term involving the difference in the two stacking energies. Asaro and Suresh [18] defined the dimensionless parameter β as $\beta = 1 - \gamma_{sf}/\gamma_{us}$ which they used in an analysis of partial dislocation emission at a nanocrystalline grain boundary; the factor $\sqrt{\mu\gamma_{us}}$ has dimensions of a stress intensity factor, namely [MPa $\cdot\sqrt{\text{m}}$]. Table 1 lists values for β for the several fcc metals studied herein, obtained from the literature and also computed from the interatomic potentials used herein. We will note in what follows the rather disparate values of γ_{us} and γ_{sf} reported and how precise quantitative predictions are often hampered. Qualitative trends are, however, quite consistent and thus definitive predictions concerning behavior are possible.

In considering Table 1 we first note that, of the four metals listed, Cu and Pd have similar shear moduli to Al and Ag. However, the parameter β is quite different between Al and Ag and modestly different between Cu and Pd. Thus, in terms of dislocation emission, one might expect rather different behavior for Al and Ag, an occurrence perhaps not surprising owing to their very different stacking fault energies, but similar behavior for Cu and Pd, despite the fact that Pd has a stacking fault energy far greater than does Cu. But how does one apply this to the process of dislocation–twin boundary interaction mediating the response of nanotwinned fcc metals? To address this, we appeal to Fig. 1c.

Asaro and Kulkarni [11] considered the process of dislocation–twin boundary interaction using models as depicted in Fig. 1c, which shows a pile up of dislocations impinging on a twin boundary as occurs, as shown below, in our molecular dynamics simulations. The pile up acts like a crack in that it concentrates stress. For the isolated,

Table 1

Shear moduli, stacking fault energies and the parameter β for various fcc metals. The values of γ_{us} , γ_{sf} and γ_{ut} were compiled from published experimental data and first principle calculations in Ref. [19]. The values of μ and the values in brackets were obtained from the interatomic potentials used in this work.

	Al	Pd	Cu	Ag
b (nm)	0.2851	0.2751	0.2556	0.2892
μ (GPa)	28	41	40	31
γ_{sf} (mJ m ⁻²)	135–200 (140)	175–180 (63)	35–78 (15)	16–22 (1)
γ_{us} (mJ m ⁻²)	175–224 (164)	265 (166)	158–210 (140)	190 (120)
γ_{ut} (mJ m ⁻²)	207 (300)	355 (230)	236 (149)	105 (120)
β	0–0.23 (0.15)	0.32–0.34 (0.62)	0.51–0.83 (0.89)	0.88–0.92 (0.99)
β_t	0.03–0.35 (0.5)	0.49–0.51 (0.72)	0.67–0.85 (0.89)	0.79–0.85 (0.99)

open-ended pile up shown, the stress intensity factor is given as:

$$K = \sqrt{2\mu n \tau_{ms} b}, \quad \text{where } n \tau_{ms} = \pi \tau_{ms}^2 \ell / (\mu b). \quad (6)$$

In Eq. (6) n represents the equilibrium number of dislocations in the pile up driven by a resolved shear stress acting on a perfect dislocation, τ_{ms} . We keep the subscripts here since Asaro and Kulkarni [11] considered the effect of general multiaxial stress states acting on disassociated dislocations. Eq. (6) also contains the pile-up length, ℓ , which scales directly with λ . To illustrate a point made earlier, we note that:

$$n = \pi \tau_{ms} \ell / (\mu b) = \pi \left(\frac{\tau_{ms}}{\mu} \right) \left(\frac{\ell}{b} \right). \quad (7)$$

If, for example, in Cu $\lambda = 15$ nm, Lu et al.'s [4] data would indicate that the normal stress levels at yield would be at the 1 GPa level. Thus $\tau_{ms} \approx 500$ MPa, and $\tau_{ms}/\mu \approx 10^{-2}$. At $\lambda = 15$ nm, $\ell \approx 17$ nm and thus $\ell/b \approx 50$. Thus $n \approx 1/2\pi \approx 1.5$. In other words, once λ falls below, say, 15 nm or so, the number of dislocations that may be accommodated is limited to a single dislocation. Thus in the context of Asaro and Kulkarni's model [11], the criteria outlined in Eq. (5) may be applied, if only as a guide, to anticipate behavior as long as $\lambda \geq 15$ nm.

With the above as a backdrop, we may proceed as follows in anticipating response at a nanotwin boundary. When groups of dislocations, roughly in an organized form of a pile up, impinge on a twin boundary, the lead dislocations will be either absorbed or transmitted as though they were being emitted from the tip of the pile up's concentrated driving force. For the lead partial, absorption or transmission is affected by γ_{us} , and of course μ . For the complete dislocation to be absorbed or transmitted, the process is affected by β as well as by μ . The partial dislocations may be "emitted" on the twin plane, i.e. absorbed, or emitted on a slip plane in the adjoining twin, i.e. transmitted. Thus we consider not only β for a slip plane, but also β_t , the analogous quantity for the twin plane. We may proceed in this manner of reasoning as long as $\lambda \geq 15$ nm.

The fact that β for Al is so low suggests that dislocations would readily be absorbed on the twin boundary. This is especially the case since as Asaro and Kulkarni [11] have shown, the transmission process through the twin boundary is more difficult due to geometric factors that favor cross-slip onto the twin plane. For Cu, however, the absorption of complete dislocations onto the twin plane is far more difficult, owing to the large values of β_t and thus either transmission or absorption is anticipated. In Ag, the expectations are similar to those for Cu. For Pd, considerations based on β alone might be inconclusive due to the intermediate value of β and β_t . However, considering the relatively high value for shear modulus, and thus of the overall stress level, adsorption and transmission are expected. This may not have been anticipated based on the rather high value of the stacking fault energy of Pd.

As described below, our simulated results are generally consistent with these expectations.

Before leaving the topic of Rice's analysis of dislocation emission from a stress concentrator such as a crack tip, we consider one additional issue, namely the distance an emitted leading partial dislocation travels just at emission, r_1 . As discussed by Asaro and Suresh [18] with the scenario depicted in Fig. 1a, upon emission the lead partial is predicted to travel a distance r_1 given by the expression:

$$\frac{r_1}{b_1} = \frac{1}{4\pi(1-\nu)\Gamma_{1us}} \frac{1}{[1-\beta^{1/2}]^2}, \quad (8)$$

where $\Gamma_{1us} = \gamma_{us}/(\mu b_1)$ is a reduced unstable stacking energy. We use this expression as a guide for estimating how far a transmitted dislocation would be expected to travel into the adjoining twin lamella. Special caution is suggested here, however, since the reliability of such forecasts is quite sensitive to the value of β , whereas the values of β are known only quite approximately at this time. One needs only to survey Table 1 to appreciate the wide disparity in the values of β extracted from various sources. In fact Eq. (8) predicts that for Al the normalized distance r_1/b_1 is only about 1.5! But for Cu the distance is of the order of 10^3 and for Pd and Ag even a factor of 5–10 larger. An implication here is that twin boundaries in Cu, Ag and Pd are expected to strongly interact via dislocation transmission and subsequent impingement on an adjacent twin, whereas in Al such interactions may be far weaker. The results from our simulations, shown in Figs. 4–6 for Pd, Cu and Ag, indicate that emitted dislocations travel at least 3 nm or more just at transmission and then expand rapidly with increasing load. It is not surprising that if twin boundaries are separated by modest distances, twin–twin interactions would be expected; such critical spacings may, indeed, be of the order of 15 nm as suggested by the recent data of Lu et al. [4]. For this reason we explore the effects of twin–twin interaction below.

3. Simulation methods and results

We performed simulations of shear and nanoindentation of bicrystals containing a coherent twin boundary (CTB). The fcc metals studied were Al, Cu, Pd and Ag. The details of the computational method and problem description are provided below.

3.1. Methods of simulation

All simulations were carried out at 0 K using the molecular dynamic code, LAMMPS [21]. The simulation cells were aligned along the $[1\bar{1}\bar{2}]$, $[110]$ and $[1\bar{1}1]$ crystallographic directions as shown by the inset in Fig. 2. Periodic boundary conditions were applied in the X - and Y -directions. The embedded atom (EAM) interatomic potentials used in this work are those by Ercolessi and Adams [22] for Al, Foiles et al. [23] for Cu and Ag, and Voter and Chen [24] for Pd.

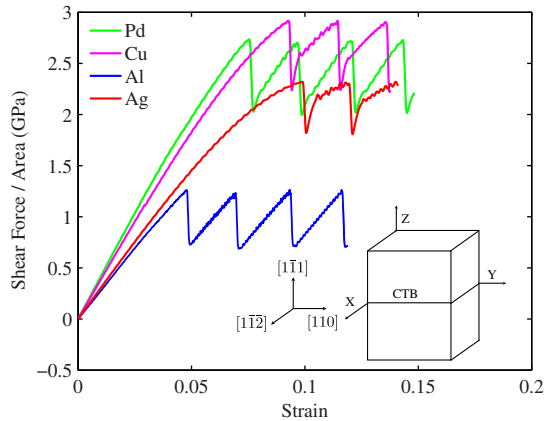


Fig. 2. The shear stress vs. strain plots for the uniform shear of a CTB in various fcc metals. The sawtooth-like behavior indicates normal motion of the CTB.

We wish to note here that the accuracy of the predictions made by atomistic simulations is intimately related to the accuracy of the empirical potentials. Our simulations were performed using potentials that qualitatively capture the trends of the parameters (β , β_t , and μ) used in our analysis, and hence are consistent with the results of our analysis and experimental observations.

The shear tests were performed on bicrystals of size $60 \times 80 \times 80 \text{ \AA}$, with the CTB located at the center and normal to the Z-direction (Fig. 2). The top surface was displaced along the $[\bar{1}12]$ direction with a velocity of 0.02 \AA ps^{-1} while the bottom surface was held fixed. The nanoindentation on a (111) surface was performed on bicrystals of size $200 \times 200 \times 100 \text{ \AA}$, consisting of about 350,000 atoms, with a spherical indenter of radius $R = 40 \text{ \AA}$. The CTB was located about 25 \AA below the indentation surface. The indenter was modeled using an external potential given by

$$\Phi^{\text{ext}}(r) = AH(R - r)(R - r)^3,$$

where A is a force constant taken to be 5 eV/\AA^3 in the present calculations, $H(r)$ is the step function, and r denotes the position vector of an atom [25]. The indentation was performed at a strain rate of $2 \times 10^9 \text{ s}^{-1}$.

3.2. Results for dislocation twin interactions

The results of the shear simulations for various fcc metals are shown in Fig. 2. In all cases, we observe a sawtooth-like behavior of the stress vs. strain curve, which corresponds, in turn, to the uniform motion of the CTB normal to the plane of the boundary, when subjected to shear in that plane. Such general behavior has been previously reported by, for example, Cahn et al. [26], Sansoz and Molinari [2], and Kulkarni et al. [8]. We note that, among the fcc metals considered herein, the CTB in Cu has the highest shear strength of $\sim 3 \text{ GPa}$, with Pd following closely at $\sim 2.7 \text{ GPa}$. Also, although Ag has a much smaller shear

modulus than either Cu or Pd, the shear strength of the CTB is quite high ($\sim 2.3 \text{ GPa}$). On the other hand, the CTB in Al has the lowest shear strength of $\sim 1.2 \text{ GPa}$. We further note that at the finite temperature of 300 K the peak stresses shown in Fig. 2 fall by approximately 20% (see Kulkarni et al. [8]) and thus all statements regarding relative behavior would hold at 300 K . The peak stresses of Fig. 2 do not simply scale with shear modulus, nor do they scale with the parameters β or β_t exclusively. Rather the combination $(\mu\beta\gamma_{\text{us}})^{1/2}$ or $(\mu\beta_t\gamma_{\text{us}})^{1/2}$, which appears prominently in Eq. (5), provides a far better guide, and forecasts the relative ranking of peak stresses to within several per cent.

The nanoindentation curves for Al, Pd, Cu and Ag are shown in Figs. 3–6, respectively. For reference, indentation force vs. indentation curves for single crystals without twins are also shown in each figure. We note that in all cases the inelastic process begins with the initiation of multiple dislocation loops under the indenter. The emitted dislocations are extended partial dislocations separated by intrinsic stacking faults. The extended dislocations impinge on the twin boundaries, and are initially absorbed into the twin boundaries. After the absorption of the first one or two dislocations, continued absorption or transmission of subsequent dislocations occurs as described below.

The insets to Figs. 3–6 show the defect structures at various indentation depths (denoted by “d”) extracted using the centrosymmetry parameter [25]. We observe that Al shows a significantly different behavior in comparison to other fcc metals in that there is profuse absorption on the CTB with no transmission seen until 20 \AA penetration. The force–indentation curve also shows some loss of hardness as compared to the single crystal. This is consistent with the low shear strength of Al CTB observed in the shear tests. Thus, our simulations also indicate that twin boundaries in Al should be the least stable and, hence, prone to significant motion that may induce grain growth.

In the case of Pd, Cu and Ag, we see both absorption and subsequent transmission of dislocations, which is in

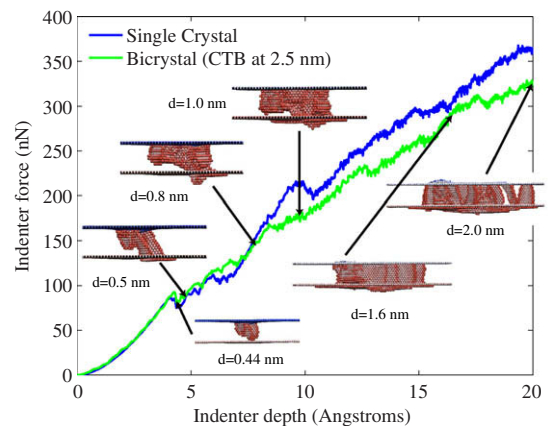


Fig. 3. Force vs. indentation depth curve for nanoindentation on a (111) surface of a bicrystal with CTB at 2.5 nm and a single crystal of Al.

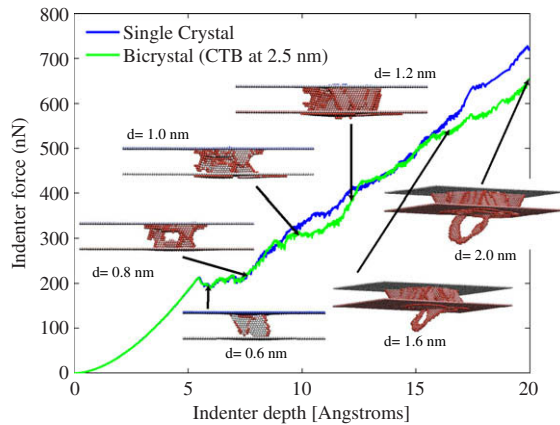


Fig. 4. Force vs. indentation depth curve for nanoindentation on a (111) surface of a bicrystal with CTB at 2.5 nm and a single crystal of Pd.

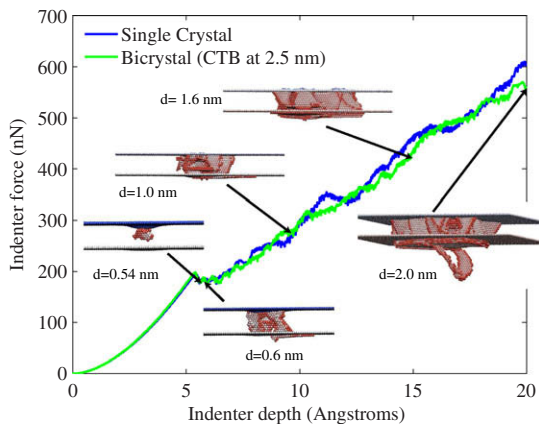


Fig. 5. Force vs. indentation depth curve for nanoindentation on a (111) surface of a bicrystal with CTB at 2.5 nm and a single crystal of Cu.

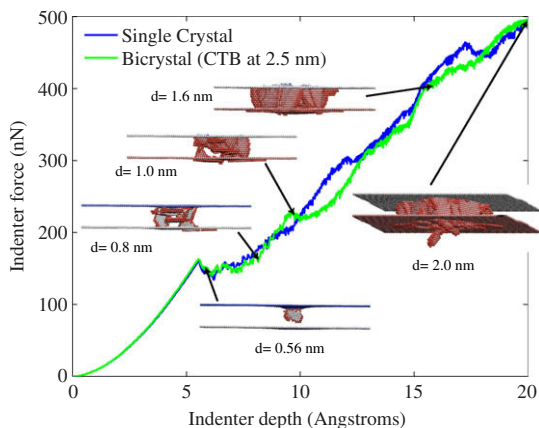


Fig. 6. Force vs. indentation depth curve for nanoindentation on a (111) surface of a bicrystal with CTB at 2.5 nm and a single crystal of Ag.

agreement with our analysis based on the parameters β and β_i and shear moduli. The contrasting behavior of Cu and Pd is of interest in that, whereas the stacking fault energy of Pd is much higher than that of Cu, the sequence of initial dislocation absorption and subsequent transmission is

similar. The indenter force is greater for Pd than for Cu at comparable indenter displacements, but the first signs of transmission occur at similar indenter forces. The defect structures are also similar. Thus the indications for Cu and Pd are that dislocation absorption is limited to the first one or two impinging dislocations and is followed by dislocation transmission. Transmission precludes normal motion of the twin boundaries and hence twin lamella coarsening. Transmission would also lead to the accumulation of dislocation debris within the twin lamella as, in fact, reported by Lu et al. [4] in twins where $\lambda \geq 15$ nm.

The behavior of Ag is most noteworthy in that the forces born by the indenter are only about 10% less than those of Pd. The defect structures are similar to those observed in either Cu or Pd. Moreover, the sequence of events regarding initial absorption and subsequent transmission are likewise similar to those observed in both Cu or Pd.

3.3. Twin–twin interactions

As noted above, Lu et al. [4] have reported the important fact that as the twin lamella thickness, λ , falls below 15 nm in Cu, the strength of the nanotwinned structure decreases with decreasing λ . The observed reduction in yield strength is by at least a factor of 2 from its peak at $\lambda \approx 15$ nm as $\lambda \rightarrow 4$ nm. Lu et al. [4] attributed this to the increase in the twin density as λ decreases, coupled to the belief that the twin boundaries contain pre-existing dislocations and hence act as shearing planes, i.e. as slip systems in themselves. That this behavior represents a continuous evolution of a single mechanism as twin density increases, or rather a transition in behavior at a critically small λ , is discussed below. Here we explore the behavior of twins in shear when the twin boundaries contain defects in the form of partial dislocations and steps caused by dislocation impingement and transmission. Twin boundaries are known to contain such defects even upon growth and certainly attain them immediately upon deformation.

For this purpose, models were created comprised of simulation blocks containing a single and two twin boundaries. The upper twin boundary was positioned 2.5 nm below the indenter surface in both models, and in the case of the simulation block with two twins, the second twin was positioned at various spacings, i.e. 10, 5 and 2.5 nm, below the upper twin. These spacings place twins such that direct interaction via transmitted dislocations may be expected, i.e. expected if the overall deformations are large enough so that transmitted defects travel from twin boundary to twin boundary. With larger twin spacings, say $\lambda \geq 15$ nm, deformation is more controlled by intratwin dislocation processes and the twin–twin interactions of this type are less important. Indentations were first performed so as to create partial dislocations and steps in the samples with a single twin, then to create such defects in only the upper twin in the samples with two twins, and finally to create defects in both twins in the second simulation block. Shear simulations as described earlier were subsequently

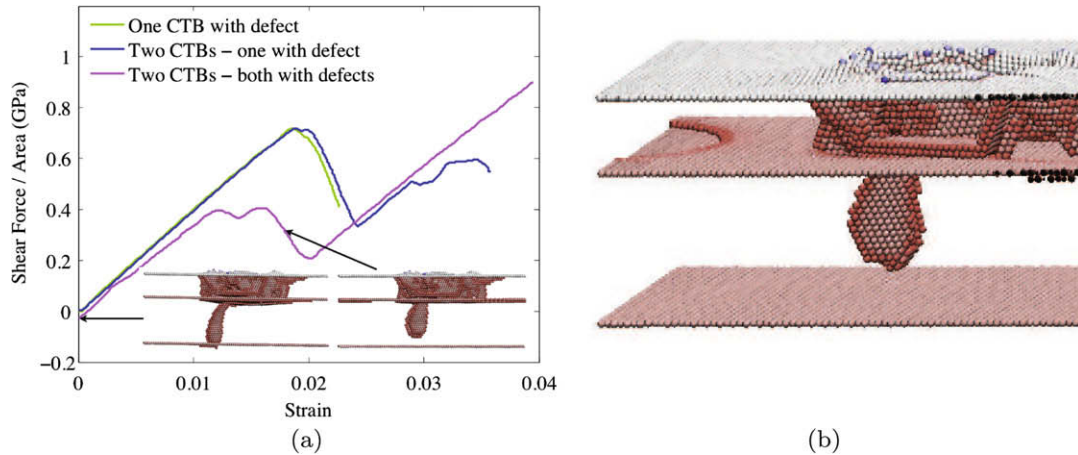


Fig. 7. (a) Shear stress vs. strain plots for the uniform shear of a Pd crystal for three cases: (i) a CTB having an absorbed dislocation, (ii) two CTBs with the upper one having an absorbed dislocation and (iii) two CTBs both having an absorbed dislocation. (b) Snapshot showing nonuniform normal motion (on the left-hand side) of the twin boundary subjected to shear. The CTBs are spaced 5 nm apart.

performed on these three deformed samples. The results of these model simulations are shown in Fig. 7a and b for Pd with a twin spacing of 5 nm, and then for Cu and Pd with twin spacings of 2.5 nm as shown in Fig. 8a and b and Fig. 9a and b, respectively.

As shown in Fig. 7a, when indentation was carried out so as to introduce defects into only the upper twin boundary, no perceptible loss in strength was observed. However, when indentation was carried out so that a single transmitted dislocation loop impinged on the lower twin boundary (see the left-hand side insert in Fig. 7a), subsequent shear revealed a significant loss in strength. The sequence of events accompanying this was itself interesting. The single dislocation loop actually receded from the lower twin boundary accompanied by a shearing of the upper twin. Fig. 7b shows the nonuniform normal motion of the twin boundary that accompanies boundary shear via a boundary dislocation loop. Similar results were observed for Cu

with a twin spacing of 5 nm as also detailed next for the case of twins spaced 2.5 nm apart.

We recall that at 0 K the peak strength of a perfect twin boundary in Cu is approximately 2.9 GPa. In the case of a single CTB containing defects, induced by the deformation of indentation, the peak stress falls to 785 MPa (see Fig. 8b). In the sample with two twin boundaries spaced 2.5 nm apart, but with defects in only the upper twin boundary, the peak stress falls a bit more to 760 MPa. Thus if the two twin boundaries interact here, this interaction is rather weak. On the other hand, when both boundaries contain defects, i.e. when the two boundaries directly interact via deformation, the peak stress falls more dramatically to 480 MPa. This effect of twin–twin interaction is similar to that just described above for Pd. We note, as we did above, that Kulkarni et al. [8] showed that the kinetics of twin boundary shear was such that a reduction of about 20% in peak stress is expected at finite temperatures

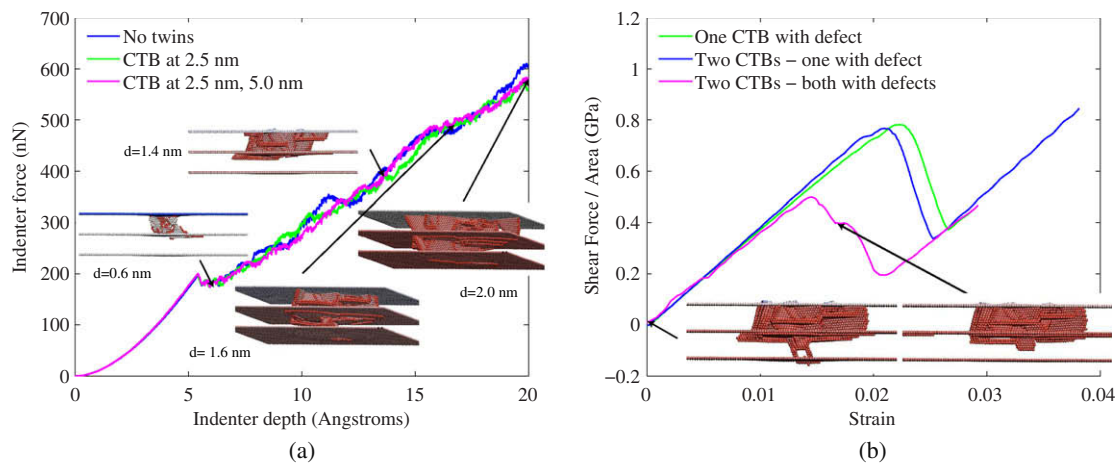


Fig. 8. (a) Force vs. indentation curve for a Cu crystal with multiple twins. (b) Shear stress vs. strain plots for the uniform shear of a Cu crystal for three cases: (i) a CTB having an absorbed dislocation, (ii) two CTBs with the upper one having an absorbed dislocation and (iii) two CTBs both having an absorbed dislocation. The CTBs are spaced 2.5 nm apart.

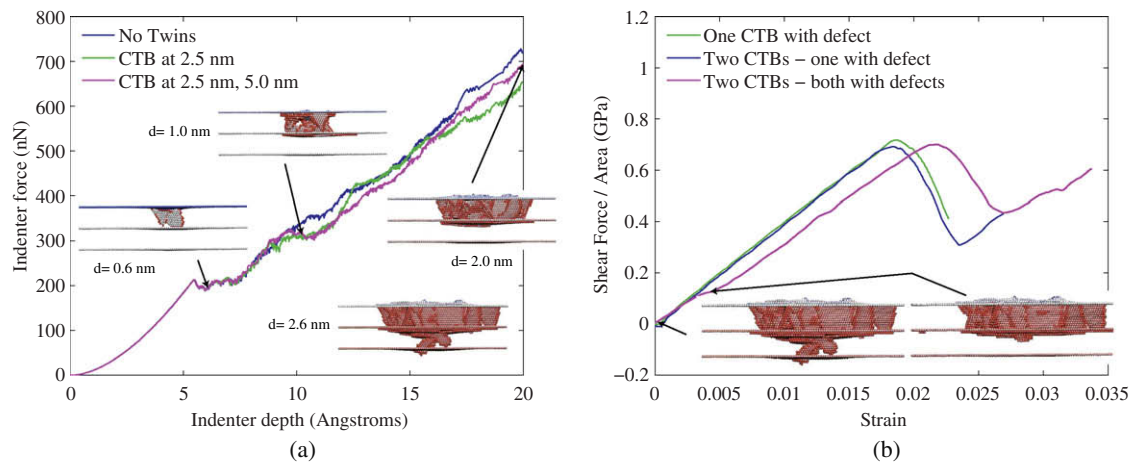


Fig. 9. (a) Force vs. indentation curve for a Pd crystal with multiple twins. (b) Shear stress vs. strain plots for the uniform shear of a Pd crystal for three cases: (i) a CTB having an absorbed dislocation, (ii) two CTBs with the upper one having an absorbed dislocation and (iii) two CTBs both having an absorbed dislocation. The CTBs are spaced 2.5 nm apart.

of 300 K, i.e. a peak stress of the order of 380 MPa is expected at 300 K. An additional reduction in peak stress is expected due to rate effects and thus at experimentally achievable strain rates, say in the range 10^{-3} s^{-1} , we indeed expect to approach the values of strength reported in experiment, i.e. 200–250 MPa.

Simulations of a similar type carried out for Pd with a twin spacing of 2.5 nm show very different trends, however. The presence of multiple twins spaced this close together tends to lead to a modest increase in hardness as measured by the load vs. indentation curve shown in Fig. 9a; the responses to shear for the three cases described above are shown in Fig. 9b. The load vs. indentation curve of Fig. 9a differs from that for Cu (Fig. 8a) in that the presence of a second CTB in proximity to another leads to a slightly higher hardness as seen at indentations beyond say 15 nm or so. Moreover, the second CTB seems to inhibit the transmission of defects through the upper CTB which begins at 2.4 nm, whereas transmission begins around 1.6 nm in the case of a single CTB (Fig. 4). This is also contrary to the observations made for Cu. At an indentation of 2.6 nm, transmitted dislocations impinge on the second CTB and begin to transmit through it. Samples were subjected to shear at $d = 0.8 \text{ nm}$ for the cases of a single CTB with defects and two CTBs with only one with defects, and at $d = 2.6 \text{ nm}$ for the case of two CTBs both with defects. As seen in Fig. 9b, with two CTBs but with defects confined to only the upper one, there is a modest decrease in strength with two CTBs as was the case for Cu. However, with defects in both CTBs the strength actually rises modestly again, in complete contrast to the case in Cu where a dramatic drop in strength was observed. In fact, we noticed an interesting effect whereby the dislocation transmitted through the second (i.e. the lower) CTB receded back into the twin lamella sandwiched between the two CTB's during shearing, creating a scenario equivalent to two CTBs but with only the first containing defects

(i.e. as in the second case). Although this reduction was also observed in Pd with twins spaced 5 nm apart, the sequence of subsequent events was quite different and was accompanied by no loss in strength. This raises the intriguing possibility that the trend of decreasing strength with lamella thickness below some critical value such as found in Cu may be resisted in Pd.

4. Discussion

Our results for the fcc metals we studied show that the behaviors of Cu, Pd and Ag are similar, and perhaps remarkably similar given their disparate stacking fault energies. The qualitative trends found in the indentation simulations followed those found in the simulations of shear of ideal twin boundaries (as in Fig. 2). For Ag and Cu, the differences scaled closely with μ (or perhaps with $(\mu\gamma_{\text{us}})^{1/2}$). Also, Ag and Cu have somewhat similar values for $\beta^{1/2}$. Pd differs slightly from Cu, due to its different value of $\beta^{1/2}$. Al, on the other hand, is distinctly different in its behavior, perhaps not surprisingly given its very different value of β . In comparison, then, one might judge nanotwinned Al to be inferior to nanotwinned Cu, Pd or Ag.

Our results also partly confirm the utility of the parameter β , or more precisely $\beta^{1/2}$, as a predictor of response (see Eq. (5)). We phrase it this way to be precise in noting how β comes into play, i.e. in the analysis of dislocation emission at a stress concentrator such as a crack tip. Only if there exists a picture such as shown in Fig. 1c can we justify this approach.

Lu et al.'s [4] observations of a transition with respect to the dependence of strength on twin lamella thickness deserves special attention. Lu et al. note, for Cu, that when $\lambda \geq 15 \text{ nm}$ the defect structure within twin lamella is characterized by dislocation tangles (see also Ref. [27]). This picture is readily envisioned by considering the entangle-

ment that would occur via the transmitted dislocations of Fig. 5. However, they report quite a different scenario when $\lambda < 15$ nm. In such cases there appears to be a direct interaction between the twin boundaries not unlike the situation shown in Fig. 8a. Their HRTEM images shown in their Fig. 4b and c indicate direct twin–twin interaction via stacking faults bridging between CTBs. Our simulations show that a result of this sort of interaction is a dramatic loss in shear strength. The experimental picture, as well as that displayed in the simulations, suggest a transition in detailed mechanism once $\lambda < 15$ nm. But can the loss of strength be described within a framework of one continuous mechanism? To explore this question, we proceed for the moment along the following, albeit phenomenological, path.

Suppose we assume that the macroscopic shearing rate, $\dot{\gamma}$, is composed of the net shearing of twin boundaries that slide at a rate v . The density of twin planes along a direction perpendicular to their planes is called ρ ; clearly, then, $\rho \propto \lambda^{-1}$. Let v be modeled by a familiar power law, $v = v_0(\tau/g)^n$, where τ is the resolved shear stress in the twin plane, g is the twin boundary “hardness”, and v_0 is a rate constant. Then, with v_0 constant:

$$\dot{\gamma} \propto \lambda^{-1} \left(\frac{\tau}{g} \right)^n \quad (9)$$

Now since when $\lambda \geq 15$ nm the strength increases with decreasing λ , we take $g = g_0 \lambda^{-\alpha}$, $\alpha > 0$. Then the proportionality in Eq. (9) becomes:

$$\dot{\gamma} \propto \lambda^{-1} \lambda^{\alpha n} \tau^n, \quad (10)$$

or at constant $\dot{\gamma}$, and constant g_0 , becomes

$$\tau \propto \lambda^{1/n-\alpha}, \quad \lambda \geq 15 \text{ nm}. \quad (11)$$

But when $\lambda < 15$ nm, we have effectively argued from above that g saturates at its value corresponding to $\lambda = 15$ nm. Thus when $\lambda < 15$ nm:

$$\tau \propto \lambda^{1/n} (15)^{-\alpha}. \quad (12)$$

Now to arrive at values for α and n consistent with the data of Lu et al. [4] (see their Fig. 3a), we must have the dual conditions:

$$\frac{1}{n} - \alpha = -\frac{1}{2}, \quad \alpha n = \frac{\ln(60/8)}{\ln(60/15)}. \quad (13)$$

These conditions are arrived at as follows: When $\lambda \geq 15$ nm, the data indicate that strength increases as approximately $\lambda^{-1/2}$; this sets the first of Eq. (13). Now consider what happens when $\lambda < 15$ nm as well as when $\lambda \geq 15$ nm. At $\lambda = 8$ nm and $\lambda = 60$ nm the strengths are equal (see Fig. 3a of Lu et al. [4]) – this leads to the second of Eq. (11). Together Eq. (13) yield:

$$\alpha \approx 1, \quad n \approx 2. \quad (14)$$

But is this reasonable? If it is, then we have provided a speculative model with proper scaling that is based on the notion that at $\lambda \geq 15$ nm and at $\lambda < 15$ nm

macroscopic deformation is mediated by twin boundary sliding. The softening effect is thereby due solely to an increase in twin density (and an accompanying saturation in twin boundary strength). Note that twin boundary sliding may be the result of the glide of absorbed dislocations. But despite the fact that the structures are very different in these two regimes of twin thickness [4], this requires that $g \propto \lambda^{-1}$! Known models and dimensional scaling argue against this. Thus the more probable situation is that the loss in strength is the result of a transition in deformation mechanism due to twin–twin interaction. We find, however, that the phenomenon of decreasing strength appears not to occur in Pd, at least for very small twin spacings.

With the above results as a backdrop, we might speculate as to the expected behavior of other fcc metals, e.g. Au and Ni. Relevant properties are shown in Table 2. For Au we expect behavior similar to that displayed by Cu or possibly Ag. When compared to Ag, however, we note that the higher values of β , β_t for Ag combined with the fact that $\mu_{\text{Ag}} > \mu_{\text{Au}}$ suggest a strength for Au somewhat less than for Ag. Ni certainly appears to resemble Pd, but with a higher shear modulus. Taken together, the results suggest that the processing of nanotwinned Ag and Pd may lead to a set of observations of significant utility and interest. For one, nanotwinned Pd would allow for the confirmation of a, most welcome, lack of transition causing serious loss in strength. Nanocrystalline Pd has been the subject of limited experimental studies, but some data does exist (e.g. [28,29]). Particularly, Rosner et al. [30] have shown that nanocrystalline Pd may be twinned when subject to strains of the order of less than 0.5 (via rolling) at ambient temperatures at modest strain rates of the order 0.3 s^{-1} . No direct studies have been made of the behavior of the nanotwinned structure produced during the rolling process, but results suggest a possible path to producing nanotwinned Pd via severe plastic deformation. For Ag, nanotwins should lead to a class of metal with high conductivity and high strength. What is also of value to consider is the fact that Ag, Pd and Cu are twinnable metals [19], in that order, and thus the prospect of synthesizing nanotwinned materials exists.

Table 2

Shear moduli, stacking fault energies and the parameter β for Au and Ni. The listed values of γ_{us} , γ_{sf} and γ_{ut} were compiled from published experimental data and first principle calculations in Refs. [19,20]. The values of μ were obtained from the interatomic potentials used in this work.

	Au	Ni
b (nm)	0.2885	0.2489
μ (GPa)	22	68
γ_{sf} (mJ m ⁻²)	30–45	110–125
γ_{us} (mJ m ⁻²)	110	273
γ_{ut} (mJ m ⁻²)	135	324
β	0.59–0.73	0.54–0.6
β_t	0.67–0.78	0.61–0.66

5. Summary

Our findings confirm the high performance of nanotwinned metals Ag, Pd, Cu, and possibly Ni and Au. To date, only Cu has been studied experimentally. Our results suggest the special utility of exploring twinned Pd and Ag in the near future for reasons outlined above. As for material parameters that may be used to forecast behavior, at least qualitatively, we find that the parameters we call β and β_t are indeed useful, albeit they should be used with caution as they are known imprecisely at present and are linked to processes occurring under specific conditions. Finally, we add that our findings and analysis add genuinely new perspectives regarding the behavior of nanotwinned fcc metals as witnessed by the fact that the recent review of Lu et al. [31] on this subject does not discuss, or raise, any of the specific issues regarding our comparisons despite itself being quite thorough and up to date.

Acknowledgements

This work was supported by the US National Science Foundation under Grant CMMI-0758561 and through TeraGrid resources provided by Texas Advanced Computing Center.

References

- [1] Sutton AP, Balluffi RW. Interfaces in crystalline materials. New York: Oxford University Press; 1995.
- [2] Sansoz F, Molinari JF. Acta Mater 2005;53:1931.
- [3] Lu L, Shen YF, Chen XH, Qian LH, Lu K. Science 2004;304:422.
- [4] Lu L, Chen X, Huang X, Lu K. Science 2009;323:607.
- [5] Zhang K, Weertman JR, Eastman JA. Appl Phys Lett 2004;85:5197.
- [6] Zhang K, Weertman JR, Eastman JA. Appl Phys Lett 2005;87:061921.
- [7] Shute CJ, Meyers BD, Xie S, Barbee TW, Hodge AM, Weertman JR. Scr Mater 2009;60:1073.
- [8] Kulkarni Y, Asaro RJ, Farkas D. Scr Mater 2008;60:532.
- [9] Lu L, Schwaiger R, Shan ZW, Dao M, Lu K, Suresh S. Acta Mater 2005;53:2169.
- [10] Dao M, Lu L, Asaro RJ, Hosson JTM, Ma E. Acta Mater 2007;55:4041.
- [11] Asaro RJ, Kulkarni Y. Scr Mater 2008;58:389.
- [12] Zhu T, Li J, Samanta A, Kim HG, Suresh S. PNAS 2007;104:3031.
- [13] Jin ZH, Gumbsch P, Ma E, Albe K, Lu K, Hahn H, et al. Scr Mater 2006;54:1163.
- [14] Dewald MP, Curtin WA. Philos Mag 2007;30:4615.
- [15] Jin ZH, Gumbsch P, Ma E, Albe K, Lu K, Gleiter H, et al. Acta Mater 2008;56:1126.
- [16] Chen Z, Jin Z, Gao H. Phys Rev B 2007;75:212104.
- [17] Rice JR. J Mech Phys Solids 1992;40:239.
- [18] Asaro RJ, Suresh S. Acta Mater 2005;53:3369.
- [19] Tadmor EB, Bernstein N. J Mech Phys Solids 2004;52:2507.
- [20] Kibey S, Liu JB, Johnson DD, Sehitoglu H. Acta Mater 2007;55:6843.
- [21] Plimpton SJ. J Comp Phys 1995;117:1.
- [22] Ercolessi F, Adams JB. Europhys Lett 1994;28:583.
- [23] Foiles SM, Baskes MI, Daw MS. Phys Rev B 1986;33:7983.
- [24] Voter AF, Chen SP. Mater Res Soc Symp Proc 1987;82:175.
- [25] Kelchner CL, Plimpton SJ, Hamilton JC. Phys Rev B 1998;58:11085.
- [26] Cahn JW, Mishin Y, Suzuki A. Acta Mater 2006;54:4953.
- [27] Wang YB, Wu B, Sui ML. Appl Phys Lett 2008;93:041906.
- [28] Neiman GW, Weertman JR. J Mater Res 1991;6:1012.
- [29] Krill CE, Birringer R. Mater Sci Forum 1996;225–227:263.
- [30] Rosner H, Markmann J, Weissmuller J. Philos Mag Lett 2004;84:321.
- [31] Lu K, Lu L, Suresh S. Science 2009;324:349.